antioxidants

MDPI

Article

Anticancer and Anti-Neuroinflammatory Constituents Isolated from the Roots of *Wasabia japonica*

Jong Eel Park [1,2], Tae Hyun Lee [1,3], Song Lim Ham [3], Lalita Subedi [4], Seong Min Hong [4], Sun Yeou Kim [4,5], Sang Un Choi [6], Chung Sub Kim [1,3,*] and Kang Ro Lee [1,*]

1 School of Pharmacy, Sungkyunkwan University, Suwon 16419, Korea; jongilpark@skku.edu (J.E.P.); thlee16@skku.edu (T.H.L.)
2 Korea Environment Corporation, 42 Hwangyeong-ro, Seo-gu, Incheon 22689, Korea
3 Department of Biopharmaceutical Convergence, Sungkyunkwan University, Suwon 16419, Korea; songlim0824@skku.edu
4 Gachon Institute of Pharmaceutical Science, Gachon University, Incheon 21936, Korea; subedilali@gmail.com (L.S.); hongsm0517@gmail.com (S.M.H.); sunnykim@gachon.ac.kr (S.Y.K.)
5 College of Pharmacy, Gachon University, #191, Hambakmoero, Yeonsu-gu, Incheon 21936, Korea
6 Korea Research Institute of Chemical Technology, Daejeon 34114, Korea; suchoi@krict.re.kr
* Correspondence: chungsub.kim@skku.edu (C.S.K.); krlee@skku.edu (K.R.L.); Tel.: +82-31-290-7750 (C.S.K.); +82-31-290-7727 (K.R.L.)

Abstract: Wasabi (*Wasabia japonica* (Miq.) Matsum.) is a pungent spice commonly consumed with sushi and sashimi. From the roots of this plant, a new 2-butenolide derivative (**1**) and 17 previously reported compounds (**2**–**18**) were isolated and structurally characterized. Their chemical structures were characterized based on the conventional NMR (^{1}H and ^{13}C, COSY, HSQC, and HMBC) and HRESIMS data analysis. All of these phytochemicals (**1**–**18**) were evaluated for their antiproliferative effects on the four human tumor cell lines (A549, SK-OV-3, SK-MEL-2, and MKN-1), for their inhibitory activity on nitric oxide (NO) production in lipopolysaccharide (LPS)-activated BV-2 microglia cells, and for their nerve growth factor (NGF)-releasing effect from C6 glioma cells. Among the isolated compounds, compound **15** showed powerful antiproliferative activities against A549 and SK-MEL-2 cell lines with IC_{50} values of 2.10 and 9.08 μM, respectively. Moreover, the new compound **1** exhibited moderate NO inhibition activity with IC_{50} value of 45.3 μM.

Keywords: *Wasabia japonica*; Brassicaceae; 2-butenolide; anticancer; anti-neuroinflammation

Citation: Park, J.E.; Lee, T.H.; Ham, S.L.; Subedi, L.; Hong, S.M.; Kim, S.Y.; Choi, S.U.; Kim, C.S.; Lee, K.R. Anticancer and Anti-Neuroinflammatory Constituents Isolated from the Roots of *Wasabia japonica*. *Antioxidants* **2022**, *11*, 482. https://doi.org/10.3390/antiox11030482

Academic Editor: Stanley Omaye

Received: 29 January 2022
Accepted: 26 February 2022
Published: 28 February 2022

1. Introduction

Wasabia japonica (Miq.) Matsum., commonly known as wasabi, is one of the most well-known species among Brassicaceae plants. This plant is a perennial plant and has been cultivated mainly in Korea and Japan. Because of their tangy taste, the roots of wasabi have long been used as a spice for sushi and sashimi. A wide range of biological studies on *W. japonica* have been investigated so far; however, most of the experiments were focused on its sulfur-containing constituents, isothiocyanates (ITCs). For examples, two major components, 6-(methylsulfinyl)hexyl isothiocyanate (6-MITC) and allyl isothiocyanate (AITC), exhibited anticancer [1–5], antioxidant [6], anti-inflammatory [7,8], neuroprotective [9], and antimicrobial [10] properties. The other minor constituents of *W. japonica* contain antioxidant phenylpropanoid [11], anticancer and anti-inflammatory monogalactosyl diacylglycerides [12], and antifungal indole derivatives [13]. However, minor bioactive components of *W. japonica* with different structural classes other than ITCs remain largely unknown.

In our continuing efforts to discover bioactive constituents from the Korean traditional medicinal plants, we have investigated the roots of *W. japonica* and isolated structurally unique thioglycosides and lignan glycosides with neurotrophic and/or anti-inflammatory

activities [14,15]. To discover anticancer compounds within non-ITCs class from this plant, we have tested antiproliferative effects of hexanes-, chloroform ($CHCl_3$)-, ethyl acetate (EtOAc)-, and *n*-butanol (*n*-BuOH)-soluble fractions of the methanol (MeOH) extract of *W. japonica* roots, and among them, the hexanes-soluble faction displayed the most potent activities with GI_{50} values of 30.57, 21.71, 16.34, and 50.64 μg/mL against A549, SK-OV-3, SK-MEL-2, and HCT-15 cancer cell lines, respectively (Table 1). Therefore, we then focused mainly on the hexanes-soluble fraction, and herein we report the isolation and structure characterization of anticancer and anti-inflammatory constituents from the *W. japonica* roots. A total 18 compounds were identified (Figure 1), and the structure of the new isolate, wasabolide (**1**), was elucidated by the conventional spectroscopic (i.e., NMR) and spectrometric (i.e., MS) data analysis.

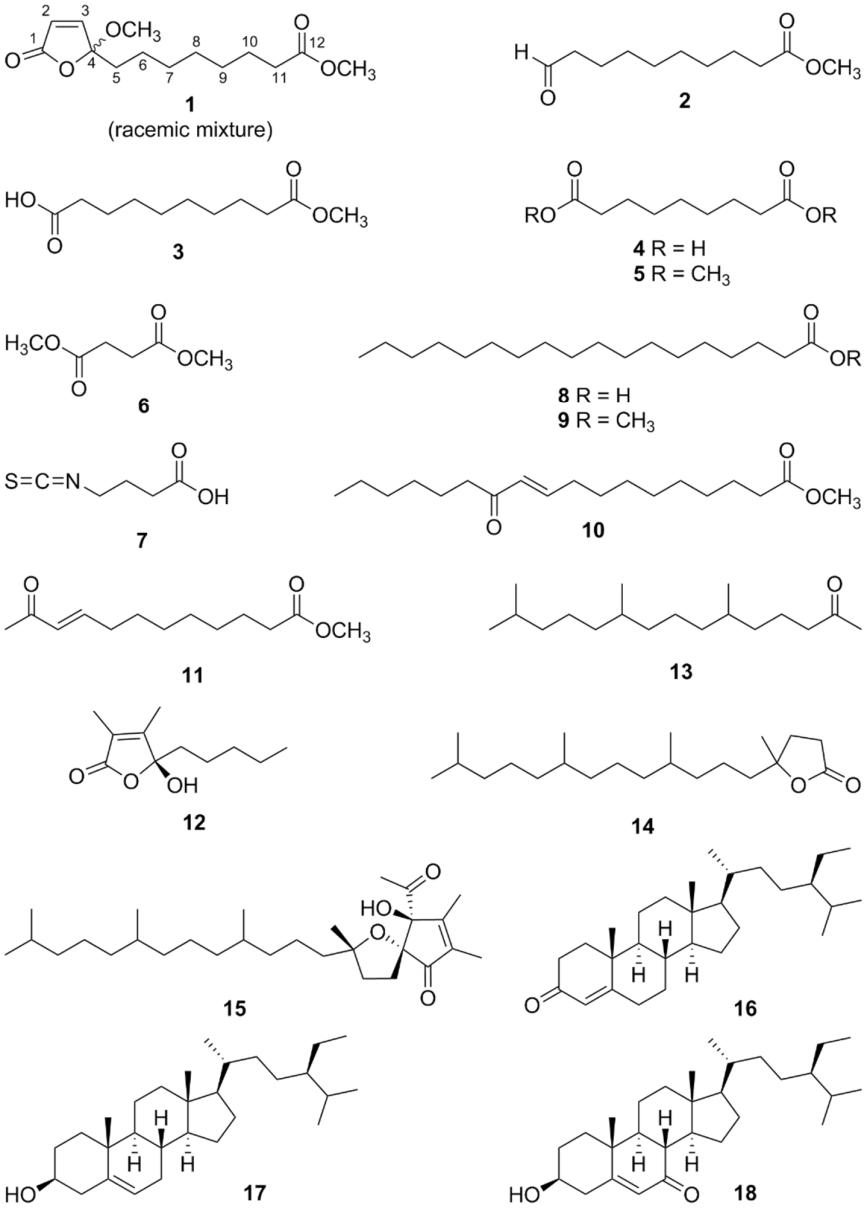

Figure 1. Chemical structure of compounds **1**–**18**.

Table 1. Antiproliferative activities of hexanes-, $CHCl_3$-, EtOAc-, and *n*-BuOH-soluble fractions of *W. japonica* MeOH extract against four cultured human cancer cell lines in the Sulforhodamine B (SRB) bioassay.

Fraction	GI_{50} (μg/mL) [1]			
	A549	**SK-OV-3**	**SK-MEL-2**	**HCT-15**
hexanes	30.57	21.71	16.34	50.64
$CHCl_3$	52.32	57.09	57.60	36.53
EtOAc	>100	>100	>100	>100
n-BuOH	>100	>100	40.01	>100

[1] Half-maximal growth inhibitory concentration; the concentration of fraction that caused a 50% inhibition in cell growth.

2. Materials and Methods

2.1. General Experimental Procedures

Bruker AVANCE III 700 NMR spectrometer at 700 MHz (^{1}H) and 175 MHz (^{13}C) was used to measure the NMR spectra (^{1}H, ^{13}C, COSY, HSQC, and HMBC) at 700 MHz (^{1}H) and 175 MHz (^{13}C) with chemical shifts given in ppm (δ) (Bruker, Karlsruhe, Germany) and the resultant spectra were processed using MestReNova (Mnova, version 14.1.2-25024). Chloroform-*d* and methanol-d_4 (Cambridge Isotope Laboratory, Inc., Tewksbury, MA, USA) were used for NMR analysis of the isolated compounds. High-resolution electrospray ionization mass spectroscopy (HRESIMS) was measured by using an Agilent 1290 Infinity II HPLC instrument (Foster City, CA, USA) coupled to a G6545B quadrupole time-of-flight (Q-TOF) mass spectrometer (Agilent Technologies, Foster City, CA, USA) with a Kinetex C_{18} 5 μm column (250 mm length × 4.6 mm i.d.; Phenomenex, Torrance, CA, USA). The semipreparative high-performance liquid chromatography (HPLC) furnished with a Gilson 306 pump (Gilson, Middleton, WI, USA), a Luna C18 10 μm column (250 mm length × 10 mm i.d.; Phenomenex, Torrance, CA, USA), an Apollo Silica 5 μm column (250 mm length × 10 mm i.d.; Apollo, Manchester, UK), and a Shodex refractive index detector (Gilson, New York, NY, USA) was used for compounds isolation. Low pressure liquid chromatography (LPLC) was performed with a LiChroprep Lobar-A Si 60 column (Merck, Darmstadt, Germany) and an FMI QSY-0 pump. Column chromatography was performed employing either silica gel 60 (70−230 and 230−400 mesh; Merck, Darmstadt, Germany) or RP-C_{18} silica gel (Merck, 230−400 mesh). Merck precoated silica gel F_{254} plates and RP-C_{18} F_{254s} plates (Merck, Darmstadt, Germany) were used for thin-layer chromatography (TLC) analysis. Spots were detected on TLC under UV light or by heating after spraying with anisaldehyde−sulfuric acid.

2.2. Plant Material

The roots of *W. japonica* (3.3 kg) were collected in Hanam, Republic of Korea, in October 2014. One of the authors, Kang Ro Lee, identified the plant, and a voucher specimen (SKKU-NPL 1409) was deposited in the herbarium of the School of Pharmacy, Sungkyunkwan University, Suwon, Republic of Korea.

2.3. Extraction and Isolation

The roots of *W. japonica* (3.3 kg) were extracted with 80% aqueous MeOH at room temperature and filtered. The crude extract was concentrated under reduced pressure to yield a MeOH extract (750 g). The extract was suspended in deionized H_2O, and then it was partitioned with hexanes (1.3 g), $CHCl_3$ (5.6 g), EtOAc (5.8 g), and *n*-BuOH (2.7 g). The hexanes-soluble fraction (1.3 g) was chromatographed on silica gel column (hexane-EtOAc, 4:1 → 1:1) to afford 20 fractions (H1-H20). Fraction H1 (100 mg) was applied to Waters Sep-pak silica Vac 6 cc (hexane-EtOAc, 1:0 → 1:1) to yield six sub-fractions (H11–H16), and compound **9** (2 mg, 0.0003%) was acquired by purifying sub-fraction H15 (10 mg), employing semipreparative silica HPLC with an isocratic mixture of hexane-EtOAc (30:1, flow rate of 2.0 mL/min). Compound **13** (3 mg, 0.0004%) was purified from the fraction H2

(35 mg), using semipreparative silica HPLC eluting with hexane-EtOAc (30:1, 2 mL/min) under isocratic conditions. Fraction H3 (35 mg) was purified by using semipreparative silica HPLC, with an isocratic mixture of hexane-EtOAc (15:1, 2 mL/min), to produce compounds **10** (3 mg, 0.0004%) and **15** (3 mg, 0.0004%). Fraction H4 (33 mg) was divided into four sub-fractions (H41–H44), using C_{18} Waters Sep-pak Vac 6 cc by eluting with 95% aqueous MeOH. Compound **16** (3 mg, 0.0004%) was isolated from sub-fraction H44 (15 mg), using semipreparative silica HPLC eluting with an isocratic mixture of hexane-EtOAc (30:1, 2 mL/min). Fraction H5 (63 mg) was subjected to C_{18} Waters Sep-pak Vac 6 cc with 95% aqueous MeOH as an eluent to acquire three sub-fractions (H51–H53). Compounds **2** (4 mg, 0.0005%) and **5** (2 mg, 0.0003%) were purified from sub-fraction H51 (40 mg). Compound **14** (2 mg, 0.0003%) was isolated by purification, using semipreparative silica HPLC eluting with an isocratic mixture of hexane–EtOAc (8:1, 2 mL/min) from sub-fraction H52 (11 mg). Fraction H6 (100 mg) was separated on a Lobar A Si 60 (240 mm × 10 mm) column ($CHCl_3$-MeOH, 500:1) to yield four sub-fractions (H61–H64). Sub-fraction H64 (19 mg) was further separated by using semipreparative silica HPLC eluting with an isocratic mixture of hexane–EtOAc (4:1, 2 mL/min) to acquire compound **17** (8 mg, 0.001%). Compound **11** (2 mg, 0.0003%) was purified from fraction H7 (13 mg) by employing semipreparative HPLC (85% aqueous MeOH, 2 mL/min) under isocratic conditions. Fraction H9 (40 mg) was separated into two sub-fractions (H91 and H92) through C_{18} Waters sep-pak Vac 6 cc by eluting with 100% MeOH, and sub-fraction H91 (15 mg) was further isolated by semipreparative HPLC (82% aqueous MeOH, 2 mL/min) under isocratic conditions to obtain compound **12** (2 mg, 0.0003%). Fraction H10 (40 mg) was applied to C_{18} Waters Sep-pak Vac 6 cc with 100% MeOH as an eluent to furnish three sub-fractions (H101–H103). Sub-fraction H101 (21 mg) was purified by semipreparative silica HPLC eluting with an isocratic mixture of hexane-EtOAc (2.5:1, 2 mL/min) to obtain compound **1** (3 mg, 0.0004%). Fraction H11 (28 mg) was isolated into three sub-fractions (H111–H113) using C_{18} Waters Sep-pak Vac 6 cc by eluting with 100% MeOH. Among the sub-fractions, compound **8** (4 mg, 0.0005%) was purified from the sub-fraction H112 through semipreparative silica HPLC eluting with an isocratic mixture of hexane-EtOAc (2.5:1, 2 mL/min). Fraction H13 (45 mg) was divided to three sub-fractions (H131–H133) by C_{18} Waters Sep-pak Vac 6 cc by eluting with 100% MeOH and compound **18** (5 mg, 0.0007%) was obtained by purification of sub-fraction H133 (16 mg), using semipreparative silica HPLC eluting with an isocratic mixture of hexane-EtOAc (1:1, 2 mL/min). The EtOAc-soluble fraction (5.8 g) was fractionated into six fractions (E1-E6) by passage over Diaion HP-20 column with step gradient solvents of MeOH-H_2O (0:1, 1:4, 2:3, 3:2, 4:1, and 1:0) as eluents. Fraction E2 (300 mg) was applied to a Lobar-A RP-18 (240 mm × 10 mm) column (20% aquous MeOH) to produce four sub-fractions (E21–E24). Sub-fraction E22 (80 mg) was further isolated into seven sub-fractions (E211–E217) through a Lobar A Si 60 (240 mm × 10 mm) column ($CHCl_3$-MeOH-H_2O, 3:1:0.15). Compound **7** (3 mg, 0.0004%) was isolated from sub-fraction E222 (15 mg) by semipreparative silica HPLC eluting with an isocratic mixture of $CHCl_3$-MeOH-H_2O (5:1:0.1, 2 mL/min). Sub-fraction E24 (30 mg) was purified by using semipreparative HPLC (10% aqueous CH_3CN, 2 mL/min) under isocratic conditions to afford compound **6** (2 mg, 0.0003%). Fraction E5 (160 mg) was chromatographed on silica gel column chromatography (EtOAc-MeOH-H_2O, 3:1:0.15 → 1:1:0.1) to furnish five sub-fractions (E51–E55). Compound **3** (4 mg, 0.0005%) was isolated by purification of sub-fraction E51 (10 mg), using semipreparative HPLC (50% aqueous MeOH, 2 mL/min) under isocratic conditions. Through the purification of sub-fraction E52 (17 mg) by using semipreparative HPLC (45% aqueous MeOH, 2 mL/min) under isocratic conditions, compound **4** (3 mg, 0.0004%) was obtained.

Wasabolide (**1**): colorless gum; ^{1}H (700 MHz) and ^{13}C (175 MHz) NMR data in chloroform-*d* (see Table 2); HRESIMS (positive-ion mode) *m/z* 271.1535 $[M + H]^+$ (calcd. for $C_{14}H_{23}O_5$, 271.1540, error = 1.8 ppm), 293.1348 $[M + Na]^+$ (calcd. for $C_{14}H_{22}NaO_5$, 293.1365, error = 3.8 ppm).

Table 2. NMR spectroscopic data of compounds **1** and MEO measured in chloroform-*d*.

Pos.	1		MEO [1]	
	δ_H, Multi. (*J* in Hz)	δ_C	δ_H, Multi. (*J* in Hz)	δ_C
1	-	170.1	-	169.98
2	6.22, d (5.7)	125.0	6.19, d (5.7)	124.75
3	7.12, d (5.7)	153.7	7.10, d (5.7)	153.53
4	-	111.4	-	111.28
5	1.89, m	37.1	1.90, m	36.98
6	1.37, m	23.3	1.23, brs; H-6–H-19	22.67–31.91; C-6–C-19
7	1.30, overlap	29.4 [2]	0.86, t; H-20	14.10; C-20
8	1.30, overlap	29.07 [2]	-	-
9	1.30, overlap	29.13 [2]	-	-
10	1.61, m	25.0	-	-
11	2.29, t (7.5)	34.2	-	-
12	-	174.4	-	-
OCH_3-4	3.22, s	51.3	3.20, s	51.11
OCH_3-12	3.66, s	51.6	-	-

[1] Adapted from the previous research [16]. [2] Exchangeable peaks.

2.4. Sulforhodamine B Colorimetric Assay

The antiproliferative activities of isolated compounds (**1**–**18**) were tested against the A549 (non-small-cell lung adenocarcinoma), SK-OV-3 (ovary malignant ascites), SK-MEL-2 (skin melanoma), HCT-15 (human colon adenocarcinoma), and MKN-1 (adenosquamous carcinoma), utilizing the SRB method as previously reported (Table 3) [17]. Etoposide (≥98%; Sigma-Aldrich, St. Lous, MO, USA) served as a positive control.

Table 3. Antiproliferative activities of selected compounds against four cultured human cell lines.

Compound	IC_{50} (μM) [1]			
	A549	SK-OV-3	SK-MEL-2	MKN-1
10	26.03	>30.0	>30.0	>30.0
11	17.95	>30.0	17.43	>30.0
14	13.28	12.86	13.04	14.17
15	2.10	13.23	9.08	10.04
16	19.21	>30.0	>30.0	>30.0
18	24.64	20.16	26.72	31.49
Etoposide [2]	1.51	1.94	1.13	3.37

[1] 50% inhibitory concentration; the concentration of compound that caused a 50% inhibition in cell growth. [2] Etoposide was used as a positive control.

2.5. Nitric Oxide (NO) Assay

The nitric oxide (NO) assay was performed analogously, as described in Reference [18]. The BV-2 cells, which were developed by V. Bocchini at the University of Perugia (Perugia, Italy), were used for this study [19,20]. The cells were seeded in a 96-well plate (4×10^4 cells/well) and incubated in the presence or absence of various doses of tested compounds (**1**–**18**). Lipopolysaccharide (LPS) (100 ng/mL) was added to all the pretreated wells, except the control one, and grown for 1 day. The produced levels of nitrite (NO_2), a soluble oxidized product of NO, was evaluated with 0.1% *N*-1-napthylethylenediamine dihydrochloride and 1% sulfanilamide in 5% phosphoric acid, aka the Griess reagent. The supernatant (50 μL) was mixed with the Griess reagent (50 μL). After 10 min, the absorbance was gauged at 570 nm. N^G-monomethyl-L-arginine (L-NMMA), as a nitric oxide synthase (NOS) inhibitor, was used as a positive control. Graded sodium nitrite solution was utilized to determine nitrite concentrations. A 3-[4,5-dimethylthiazol-2-yl]-2,5-diphenyltetrazolium bromide (MTT) assay was used for the cell-viability assay (Table 4).

Table 4. Effects of select compounds on NO generation in LPS-stimulated BV-2 cells.

Compound	IC_{50} (μM) [1]	Cell Viability (%) [2]
1	45.3	112.07 ± 4.78
5	90.0	98.31 ± 11.14
11	59.6	67.91 ± 4.06
15	92.4	120.77 ± 8.20
L-NMMA [3]	21.4	104.56 ± 4.20

[1] IC_{50} value of each compound was defined as the concentration (μM) that caused 50% inhibition of NO production in LPS-activated BV-2 cells. [2] Cell viability after treatment with 20 μM of each compound was determined by 3-[4,5-dimethylthiazol-2-yl]-2,5-diphenyltetrazolium bromide (MTT) assay and is expressed in percentage (%). The results are averages of three independent experiments, and the data are expressed as mean ± SD. [3] N^G-monomethyl-L-arginine (L-NMMA) was used as a positive control.

2.6. Nerve Growth Factor (NGF) Assay

The nerve growth factor (NGF) assay was performed analogously, as described in Reference [21]. C6 glioma cell lines were used to measure the NGF of the culture medium containing 10% fetal bovine serum (FBS) and 1% penicillin–streptomycin (PS) in 5% CO_2 incubator. The cells were seeded in a 24-well culture plate (1×10^5 cells/well) and incubated for 24 h. The cells were treated with or without 20 μM of the compounds (**1**–**18**), together with serum-free Dulbecco's modified Eagle's medium (DMEM) for another 24 h. Released NGF levels from the supernatants from each cell were measured by using an ELISA development kit (R&D System, Minneapolis, MN, USA). Moreover, the cell viability was evaluated by using MTT assay; 6-shogaol used as a positive control, and the results are expressed as percentage of the control group.

3. Results and Discussion

3.1. Structure Elucidation of Compounds **1**–**18**

Wasabolide (**1**) was obtained as a colorless gum, and its molecular formula was established as $C_{14}H_{22}O_5$ from the protonated and sodiated molecular ions at *m/z* 271.1535 $[M + H]^+$ (calcd. for $C_{14}H_{23}O_5^+$, 271.1540, error = 1.8 ppm) and 293.1348 $[M + Na]^+$ (calcd. for $C_{14}H_{22}NaO_5^+$, 293.1359, error = 3.8 ppm), respectively, in the HRESIMS data (Figure S1). The ^{1}H NMR spectrum of **1** (Figure S2) suggested the presence of two olefinic [δ_H 7.12 (1H, d, *J* = 5.7 Hz, H-3) and 6.22 (1H, d, *J* = 5.7 Hz, H-2)], two methoxy [δ_H 3.66 (3H, s, OCH_3-12) and 3.22 (3H, s, OCH_3-4)], and seven methylene [δ_H 2.29 (2H, t, *J* = 7.5 Hz, H-11), 1.89 (2H, m, H-5), 1.61 (2H, m, H-10), 1.37 (2H, m, H-6), and 1.30 (6H, overlap, H-7–H-9)] protons in **1**. The ^{13}C NMR spectrum of **1** (Figure S3) showed total 14 resonances, which was consistent with HRESIMS data mentioned above, including two ester/carboxylic acid(s) (δ_C 174.4 (C-12) and 170.1 (C-1)), two double bond [δ_C 153.7 (C-3) and 125.0 (C-2)], a deoxygenated [δ_C 111.4 (C-4)], two methoxy [δ_C 51.6 (OCH_3-12) and 51.3 (OCH_3-4)], and seven methylene [δ_C 37.1 (C-5), 34.2 (C-11), 29.4 (C-7), 29.13 (C-9), 29.07 (C-8), 25.0 (C-10), and 23.3 (C-6)] carbon peaks. To elucidate the planar structure of **1**, 2D NMR data of **1** including COSY, HSQC, and HMBC (Figures S4–S6) were obtained and analyzed. The presence of an α,β-unsaturated γ-butyrolactone (UBL, = 2-butenolide) moiety in **1** was suggested by observing COSY correlation between H-2 and H-3 and HMBC cross-peaks between H-2/H-3 and C-1 and H-2/H-3/H-5 and C-4 (Figure 2A). The HMBC correlation between OCH_3-4 and C-4 indicated a methoxy group located at the γ-position of UBL moiety (Figure 2A). In addition, an unusually smaller coupling constant between the *cis*-oriented two olefinic protons H-2 and H-3, 5.7 Hz, was observed. The similar *J* value has been reported from other UBL-containing organic molecules [16,22,23], supporting the presence of UBL functionality in **1**. The remaining COSY correlations between H-6 and H-5/H-7 and H-10 and H-9/H-11 and HMBC cross-peaks between H-5 and C-6, H-11 and C-9/C-10/C-12, and OCH_3-12 and C-12 indicated the presence of a fully saturated aliphatic chain with a terminal methyl ester group as the other substructure of **1**. Therefore, the planar structure of **1** was determined as in Figure 1. The most structurally similar molecule to **1** was found to be 4-methoxy-2-eicosen-4-olide (MEO) isolated from a marine sponge

(Figure 2B, right) [16] by the literature search, using SciFinder. MEO shared most of the NMR features, with **1** especially at the UBL functionality (Table 2 and Figure 2B), thus supporting our structural assignment of **1**. Finally, it was concluded that **1** was a racemic mixture based on the almost zero value of specific rotation and no Cotton effect observation in electronic circular dichroism (ECD) spectrum of **1**.

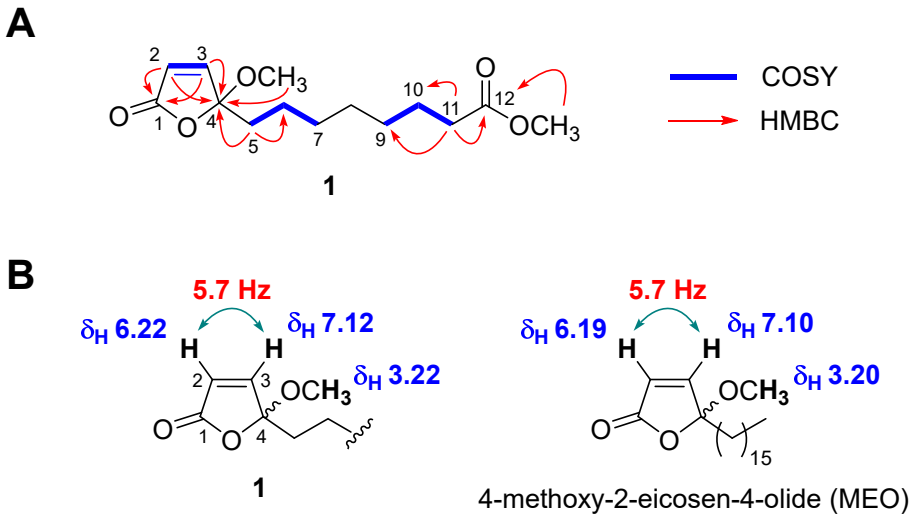

Figure 2. Structure elucidation of **1**. (**A**) Key COSY and HMBC correlation of **1**. (**B**) Comparison of the key ^{1}H NMR data around the UBL functionality in **1** (left) and its structurally similar marine metabolite MEO (right).

The 17 known compounds **2**–**18** were identified as methyl 10-oxodecanoate (**2**) [24], monomethyl sebacate (**3**) [25], azelaic acid (**4**) [26],dimethyl azelate (**5**) [26], dimethyl succinate (**6**) [27], 4-isothiocyanatobutanoic acid (**7**) [28], octadecanoic acid (**8**) [29], methyl stearate (**9**) [30], (10*E*)-12-oxo-10-octadecenoic acid methyl ester (**10**) [31], methyl 11-oxo-9-dodecenoate (**11**) [32], (*S*)-5-hydroxy-3,4-dimethyl-5-pentylfuran-2(5*H*)-one (**12**) [33], 6,10,14-Trimethyl-2-pentadecanone (**13**) [34], 5-methyl-5-(4,8,12-trimethyl-tridecyl)-dihydrofuran-2-one (**14**) [35], α-tocospiro A (**15**) [36], stigmast-4-en-3-one (**16**) [37], β-sitosterol (**17**) [38], and 7-oxo-β-sitosterol (**18**) [39] by comparing their spectroscopic data (Figures S7–S24) with those in the literature.

3.2. Biosynthetic Proposal of the New Compound **1**

Upon the structural characterization of the new metabolite **1**, its biosynthetic pathway was proposed as described below (Figure 3). First, one unit of acetyl-CoA and five units of malonyl-CoA could form the C12-fatty acid **i** with a double bond and a carbonyl group at α, β- and γ-position, respectively, which reaction resembled typical fatty acid biosynthesis. Then, oxidation of the terminal methyl group in **i** to carboxylic acid could afford dicarboxylic acid **ii** [40,41]. Geometrical isomerization could occur in **ii** that transforms the *E*- to *Z*-configuration of the double bond to yield **iii**. A hemi-acetalization reaction on **iii** could produce **iv** [22,42], which contains UBL moiety, and, finally, **1** could be formed by *O*-methylation at both hydroxy and carboxylic groups in **iv**.

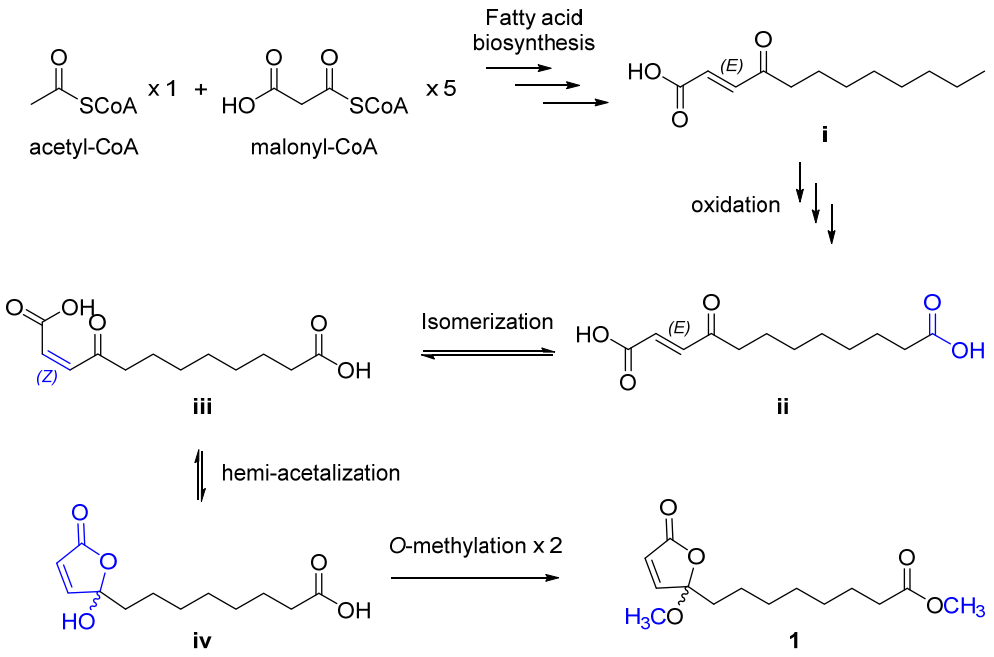

Figure 3. Plausible biosynthetic pathway of **1**.

3.3. Antiproliferative Activity of the Isolated Compounds (**1**–**18**)

In line with the potent antiproliferative activity of the hexanes-soluble fraction mentioned above, the isolated compounds (**1**–**18**) were evaluated for their antiproliferative activity against four human tumor cell lines, namely A549 (non-small cell lung adenocarcinoma), SK-OV-3 (ovary malignant ascites), SK-MEL-2 (skin melanoma), and MKN-1 (adenosquamous carcinoma), by SRB assay. Compounds **10**, **11**, **14**–**16**, and **18** isolated from the hexanes-soluble fraction strongly inhibited proliferation in cancer cell lines with different selectivity (Table 3). In detail, α-tocospiro A (**15**) showed potent activity against A549 cell line with IC_{50} value of 2.10 μM, which was comparable to that of the positive control substance, etoposide (1.51 μM). While the chemical structures of **13**–**15** are similar in that these three molecules had the same C15 fully saturated farnesyl unit, we observed no and weaker activity of **13** (IC_{50} > 20 μM) and **14** (IC_{50} = 13.28 μM), respectively, on the same cancer cell line. These data suggested that the bulky spirobicyclic moiety in α-tocospiro A (**15**) would play an important role in exhibiting antiproliferative activities in A549 cell line. Interestingly, Yuan et al. reported that α-tocospiro A (**15**) had no inhibitory activity on the A549 proliferation (IC_{50} > 20 μM) [43], but we observed the significant potency of α-tocospiro A (**15**) in this study. Moreover, α-tocospiro A (**15**) also displayed a strong antiproliferative effect on SK-OV-2, SK-MEL-2, and MKN-1 cell lines, with IC_{50} values ranging from 9.08 to 13.23 μM. Compounds **10**, **11**, **14**, **16**, and **18** showed antiproliferative activities on several cancer cell lines with IC_{50} values between 12.86 to 26.72 μM. The other compounds were inactive (IC_{50} > 30 μM).

3.4. Anti-Neuroinflammatory Activity of the Isolated Compounds (**1**–**18**)

The potential anti-neuroinflammatory effects of the isolates (**1**−**18**) were tested by measuring the level of NO production in LPS-stimulated BV-2 microglia cells. As shown in Table 4, among the tested phytochemicals, the new compound **1** showed the strongest inhibitory activity on the NO production, with an IC_{50} value of 45.3 μM and without significant cell toxicity up to 20 μM. Compounds **5**, **11**, and **15** also exhibited weak activity with IC_{50} value of 90.0, 59.6, and 92.4 μM, respectively. The other compounds were inactive (IC_{50} > 100 μM).

3.5. Neurotrophic Activity of the Isolated Compounds (**1–18**)

Lastly, the neurotrophic effect of compounds **1–18** was also evaluated, and compound **17** displayed a weak effect on NGF release from C6 cells, with a stimulation level of 107.51 ± 5.38%, compared to the positive control substance, 6-shogaol (149.53 ± 5.38%). The other compounds were inactive (stimulation level < 100%).

4. Conclusions

From the roots of *W. japonica*, a total 18 compounds (**1–18**), including a new phytochemical (**1**), were isolated by chromatographic methods and identified by spectroscopic and spectrometric data analysis, including 1D and 2D NMR and HRMS. The structure of the new compound **1** was assigned as a possibly dicarboxylic acid–derived 2-butenolide derivative and its biosynthetic pathway was also proposed based on the assigned structure and related literature search. Compound **1** showed strong anti-neuroinflammatory activity by inhibiting NO production in LPS-stimulated BV-2 cells and α-tocospiro A (**15**) exhibited a potent antiproliferative activity against A549 non-small cell lung adenocarcinoma cells.

Supplementary Materials: The following are available online at https://www.mdpi.com/article/10.3390/antiox11030482/s1. Figure S1: HRESIMS spectrum of **1**. Figures S2–S6: 1D and 2D NMR spectra of **1**. Figures S7–S34: ^{1}H and/or ^{13}C NMR spectra of **2–18**.

Author Contributions: J.E.P. performed the experiments, analyzed the data, and wrote the manuscript; T.H.L., S.L.H., and L.S. performed the experiments and analyzed the data; S.M.H., S.Y.K., and S.U.C. oversaw the biological assays; C.S.K. and K.R.L. conceived the study, oversaw experiments, and wrote the manuscript. All authors have read and agreed to the published version of the manuscript.

Funding: This work was supported by the National Research Foundation (NRF) of Korea grant funded by the government of Korea (MSIT) (Nos. 2012M3A9C4048775 and 2021R1C1C1011045), by a grant from the KRIBB Research Initiative Program, and by the BK21 FOUR Project.

Institutional Review Board Statement: Not applicable.

Informed Consent Statement: Not applicable.

Data Availability Statement: Data is contained within the article or Supplementary Materials.

Conflicts of Interest: The authors declare no conflict of interest.

References

1. Manesh, C.; Kuttan, G. Effect of naturally occurring allyl and phenyl isothiocyanates in the inhibition of experimental pulmonary metastasis induced by B16F-10 melanoma cells. *Fitoterapia* **2003**, *74*, 355–363. [CrossRef]
2. Lee, M.-J.; Tseng, W.-S.; Lai, J.C.-Y.; Shieh, H.-R.; Chi, C.-W.; Chen, Y.-J. Differential pharmacological activities of oxygen numbers on the sulfoxide moiety of wasabi compound 6-(methylsulfinyl) hexyl isothiocyanate in human oral cancer cells. *Molecules* **2018**, *23*, 2427. [CrossRef] [PubMed]
3. Yano, S.; Wu, S.; Sakao, K.; Hou, D.X. Wasabi 6-(methylsulfinyl) hexyl isothiocyanate induces apoptosis in human colorectal cancer cells through p53-independent mitochondrial dysfunction pathway. *BioFactors* **2018**, *44*, 361–368. [CrossRef] [PubMed]
4. Fuke, Y.; Hishinuma, M.; Namikawa, M.; Oishi, Y.; Matsuzaki, T. Wasabi-derived 6-(methylsulfinyl) hexyl isothiocyanate induces apoptosis in human breast cancer by possible involvement of the NF-κB pathways. *Nutr. Cancer* **2014**, *66*, 879–887. [CrossRef] [PubMed]
5. Chen, Y.-J.; Huang, Y.-C.; Tsai, T.-H.; Liao, H.-F. Effect of wasabi component 6-(methylsulfinyl) hexyl isothiocyanate and derivatives on human pancreatic cancer cells. *Evid. Based Complement. Altern. Med.* **2014**, *2014*, 494739. [CrossRef]
6. Mizuno, K.; Kume, T.; Muto, C.; Takada-Takatori, Y.; Izumi, Y.; Sugimoto, H.; Akaike, A. Glutathione biosynthesis via activation of the nuclear factor E2–related factor 2 (Nrf2)–antioxidant-response element (ARE) pathway is essential for neuroprotective effects of sulforaphane and 6-(methylsulfinyl) hexyl isothiocyanate. *J. Pharmacol. Sci.* **2011**, *115*, 320–328. [CrossRef]
7. Lohning, A.; Kidachi, Y.; Kamiie, K.; Sasaki, K.; Ryoyama, K.; Yamaguchi, H. 6-(methylsulfinyl) hexyl isothiocyanate (6-MITC) from Wasabia japonica alleviates inflammatory bowel disease (IBD) by potential inhibition of glycogen synthase kinase 3 beta (GSK-3β). *Eur. J. Med. Chem.* **2021**, *216*, 113250. [CrossRef]
8. Kim, M.W.; Choi, S.; Kim, S.Y.; Yoon, Y.S.; Kang, J.-H.; Oh, S.H. Allyl isothiocyanate ameliorates dextran sodium sulfate-induced colitis in mouse by enhancing tight junction and mucin expression. *Int. J. Mol. Sci.* **2018**, *19*, 2025. [CrossRef] [PubMed]
9. Subedi, L.; Venkatesan, R.; Kim, S.Y. Neuroprotective and anti-inflammatory activities of allyl isothiocyanate through attenuation of JNK/NF-κB/TNF-α signaling. *Int. J. Mol. Sci.* **2017**, *18*, 1423. [CrossRef] [PubMed]

10. Ko, M.-O.; Kim, M.-B.; Lim, S.-B. Relationship between chemical structure and antimicrobial activities of isothiocyanates from cruciferous vegetables against oral pathogens. *J. Microbiol. Biotechnol.* **2016**, *26*, 2036–2042. [CrossRef]
11. Hosoya, T.; Yun, Y.S.; Kunugi, A. Antioxidant phenylpropanoid glycosides from the leaves of *Wasabia japonica*. *Phytochemistry* **2008**, *69*, 827–832. [CrossRef]
12. Weil, M.J.; Zhang, Y.; Nair, M.G. Tumor cell proliferation and cyclooxygenase inhibitory constituents in horseradish (*Armoracia rusticana*) and Wasabi (*Wasabia japonica*). *J. Agric. Food. Chem.* **2005**, *53*, 1440–1444. [CrossRef]
13. Pedras, M.S.C.; Sorensen, J.L.; Okanga, F.I.; Zaharia, I.L. Wasalexins A and B, new phytoalexins from wasabi: Isolation, synthesis, and antifungal activity. *Bioorg. Med. Chem. Lett.* **1999**, *9*, 3015–3020. [CrossRef]
14. Kim, C.S.; Oh, J.; Subedi, L.; Kim, S.Y.; Choi, S.U.; Lee, K.R. Rare thioglycosides from the roots of *Wasabia japonica*. *J. Nat. Prod.* **2018**, *81*, 2129–2133. [CrossRef] [PubMed]
15. Kim, C.S.; Subedi, L.; Kwon, O.W.; Park, H.B.; Kim, S.Y.; Choi, S.U.; Lee, K.R. Wasabisides A–E, lignan glycosides from the roots of *Wasabia japonica*. *J. Nat. Prod.* **2016**, *79*, 2652–2657. [CrossRef] [PubMed]
16. Miller, M.; Hegedus, L.S. Synthesis of optically active butenolides via chromium alkoxycarbene complexes: Total synthesis of (+)-tetrahydrocerulenin and two butenolides from the marine sponge *Plakortis lita*. *J. Org. Chem.* **1993**, *58*, 6779–6785. [CrossRef]
17. Skehan, P.; Storeng, R.; Scudiero, D.; Monks, A.; McMahon, J.; Vistica, D.; Warren, J.T.; Bokesch, H.; Kenney, S.; Boyd, M.R. New colorimetric cytotoxicity assay for anticancer-drug screening. *JNCI J. Natl. Cancer Inst.* **1990**, *82*, 1107–1112. [CrossRef]
18. Kim, C.S.; Oh, J.; Suh, W.S.; Jang, S.W.; Subedi, L.; Kim, S.Y.; Choi, S.U.; Lee, K.R. Investigation of chemical constituents from *Spiraea prunifolia* var. *simpliciflora* and their biological activities. *Phytochem. Lett.* **2017**, *22*, 255–260. [CrossRef]
19. Blasi, E.; Barluzzi, R.; Bocchini, V.; Mazzolla, R.; Bistoni, F. Immortalization of murine microglial cells by a v-raf/v-myc carrying retrovirus. *J. Neuroimmunol.* **1990**, *27*, 229–237. [CrossRef]
20. Choi, Y.; Lee, M.K.; Lim, S.Y.; Sung, S.H.; Kim, Y.C. Inhibition of inducible NO synthase, cyclooxygenase-2 and interleukin-1β by torilin is mediated by mitogen-activated protein kinases in microglial BV2 cells. *Br. J. Pharmacol.* **2009**, *156*, 933–940. [CrossRef]
21. Kim, C.S.; Subedi, L.; Oh, J.; Kim, S.Y.; Choi, S.U.; Lee, K.R. Bioactive triterpenoids from the twigs of *Chaenomeles sinensis*. *J. Nat. Prod.* **2017**, *80*, 1134–1140. [CrossRef] [PubMed]
22. Mansoor, T.A.; Hong, J.; Lee, C.-O.; Sim, C.J.; Im, K.S.; Lee, D.S.; Jung, J.H. New cytotoxic metabolites from a marine sponge *Homaxinella* sp. *J. Nat. Prod.* **2004**, *67*, 721–724. [CrossRef] [PubMed]
23. De Guzman, F.S.; Schmitz, F.J. Peroxy aliphatic esters from the sponge *Plakortis lita*. *J. Nat. Prod.* **1990**, *53*, 926–931. [CrossRef]
24. Cravotto, G.; Calcio Gaudino, E.; Barge, A.; Binello, A.; Albertino, A.; Aghemo, C. Synthesis of 1-octacosanol and GC-C-IRMS discrimination of samples from different origin. *Nat. Prod. Res.* **2010**, *24*, 428–439. [CrossRef]
25. Khlebnikova, T.B.; Pai, Z.P.; Fedoseeva, L.A.; Mattsat, Y.V. Catalytic oxidation of fatty acids. II. Epoxidation and oxidative cleavage of unsaturated fatty acid esters containing additional functional groups. *React. Kinet. Catal. Lett.* **2009**, *98*, 9–17. [CrossRef]
26. Zimmermann, F.; Meux, E.; Mieloszynski, J.-L.; Lecuire, J.-M.; Oget, N. Ruthenium catalysed oxidation without CCl4 of oleic acid, other monoenic fatty acids and alkenes. *Tetrahedron Lett.* **2005**, *46*, 3201–3203. [CrossRef]
27. Dawar, P.; Raju, M.B.; Ramakrishna, R.A. One-pot esterification and Ritter reaction: Chemo-and regioselectivity from tert-butyl methyl ether. *Tetrahedron Lett.* **2011**, *52*, 4262–4265. [CrossRef]
28. Radulović, N.; Dekić, M.; Stojanović-Radić, Z. A new antimicrobial glucosinolate autolysis product, 4-isothiocyanatobutanoic acid, from the diffuse wallflower (*Erysimum diffusum*): Methyl 4-isothiocyanatobutanoate, a long unrecognized artifact of the isolation procedure? *Food Chem.* **2011**, *129*, 125–130. [CrossRef]
29. Liu, X.Q.; Baek, W.-S.; Ahn, D.-K.; Choi, H.-Y.; Yook, C.-S. The constituents of the aerial part of *Gastrodia elata* Blume. *Nat. Prod. Sci.* **2002**, *8*, 137–140.
30. Crosignani, S.; White, P.D.; Linclau, B. Polymer-supported *O*-alkylisoureas: Useful reagents for the *O*-alkylation of carboxylic acids. *J. Org. Chem.* **2004**, *69*, 5897–5905. [CrossRef]
31. Frankel, E.N.; Garwood, R.F.; Khambay, B.P.; Moss, G.P.; Weedon, B.C. Stereochemistry of olefin and fatty acid oxidation. Part 3. The allylic hydroperoxides from the autoxidation of methyl oleate. *J. Chem. Soc. Perkin Trans.* **1984**, 2233–2240. [CrossRef]
32. Lin, D.; Zhang, J.; Sayre, L.M. Synthesis of six epoxyketooctadecenoic acid (EKODE) isomers, their generation from nonenzymatic oxidation of linoleic acid, and their reactivity with imidazole nucleophiles. *J. Org. Chem.* **2007**, *72*, 9471–9480. [CrossRef] [PubMed]
33. Zhang, J.; Liang, Y.; Liao, X.-J.; Deng, Z.; Xu, S.-H. Isolation of a new butenolide from the South China Sea gorgonian coral *Subergorgia suberosa*. *Nat. Prod. Res.* **2014**, *28*, 150–155. [CrossRef] [PubMed]
34. Yildizhan, S.; van Loon, J.; Sramkova, A.; Ayasse, M.; Arsene, C.; ten Broeke, C.; Schulz, S. Aphrodisiac pheromones from the wings of the small cabbage white and large cabbage white butterflies, *Pieris rapae* and *Pieris brassicae*. *ChemBioChem* **2009**, *10*, 1666–1677. [CrossRef] [PubMed]
35. De Shan, M.; An, T.Y.; Hu, L.H.; Chen, Z.L. Diterpene derivative and chromone from *Hypericum perforatum*. *Nat. Prod. Res.* **2004**, *18*, 15–19. [CrossRef]
36. Chiang, Y.-M.; Kuo, Y.-H. Two novel α-tocopheroids from the aerial roots of *Ficus microcarpa*. *Tetrahedron Lett.* **2003**, *44*, 5125–5128. [CrossRef]
37. Della Greca, M.; Monaco, P.; Previtera, L. Stigmasterols from *Typha latifolia*. *J. Nat. Prod.* **1990**, *53*, 1430–1435. [CrossRef]
38. Chang, Y.C.; Chang, F.R.; Wu, Y.C. The constituents of *Lindera glauca*. *J. Chin. Chem. Soc.* **2000**, *47*, 373–380. [CrossRef]

39. Pettit, G.R.; Numata, A.; Cragg, G.M.; Herald, D.L.; Takada, T.; Iwamoto, C.; Riesen, R.; Schmidt, J.M.; Doubek, D.L.; Goswami, A. Isolation and structures of schleicherastatins 1−7 and schleicheols 1 and 2 from the teak forest medicinal tree *Schleichera oleosa*. *J. Nat. Prod.* **2000**, *63*, 72–78. [CrossRef]
40. Liu, L.; Zhou, S.; Deng, Y. The 3-ketoacyl-CoA thiolase: An engineered enzyme for carbon chain elongation of chemical compounds. *Appl. Microbiol. Biotechnol.* **2020**, *104*, 8117–8129. [CrossRef]
41. Han, L.; Peng, Y.; Zhang, Y.; Chen, W.; Lin, Y.; Wang, Q. Designing and creating a synthetic omega oxidation pathway in *Saccharomyces cerevisiae* enables production of medium-chain α, ω-dicarboxylic acids. *Front. Microbiol.* **2017**, *8*, 2184. [CrossRef] [PubMed]
42. Teichert, A.; Lübken, T.; Schmidt, J.; Porzel, A.; Arnold, N.; Wessjohann, L. Unusual bioactive 4-oxo-2-alkenoic fatty acids from *Hygrophorus eburneus*. *Z. Naturforsch.* **2005**, *60b*, 25–32. [CrossRef]
43. Yuan, Z.; Duan, H.; Xu, Y.; Wang, A.; Gan, L.; Li, J.; Liu, M.; Shang, X. α-Tocospiro C, a novel cytotoxic α-tocopheroid from *Cirsium setosum*. *Phytochem. Lett.* **2014**, *8*, 116–120. [CrossRef]